Segmentation of Echocardiographic Image Sequences Using Spatio-temporal Information

Einar Brandt, Lars Wigström, and Bengt Wranne

Department of Medicine and Care
Clinical Physiology, Linköping University, Sweden
einbr@imv.liu.se

Abstract. This paper describes a new method for improving border detection in image sequences by including both spatial and temporal information. The method is based on three dimensional quadrature filters for estimating local orientation. A simplification that gives a significant reduction in computational demand is also presented. The border detection framework is combined with a segmentation algorithm based on active contours or 'snakes', implemented using a new optimization relaxation that can be solved to optimality using dynamical programming. The aim of the study was to compare segmentation performance using gradient based border detection and the proposed border detection algorithm using spatio-temporal information. Evaluation is performed both on a phantom and *in-vivo* data from five echocardiographic short axis image sequences. It could be concluded that when temporal information was included weak and incomplete boundaries could be found where gradient based border detection failed. Otherwise there was no significant difference in performance between the new proposed method and gradient based border detection.

1 Introduction

Endocardial delineation in echocardiographic images could be a strong clinical tool for quantification of wall motion abnormalities and global ventricular function. Manual delineation is however very time consuming and operator dependent [1]. Automatic processing of echocardiographic data is difficult due to the poor image quality of echocardiographic images. The most important degradation mechanisms include sidelobes and grating lobes, blur, acquisition on polar coordinates, poor contrast, artifacts and speckle noise [2].

Several methods and approaches for segmenting echocardiographic image sequences have been suggested, such as active contours [3], probabilistic frameworks [2], mathematical morphology [4], simulated annealing [5], combining edge-based deformable models and region-based segmentation [6], and using M-mode echocardiograms [7]. Despite all these efforts automatic segmentation remains as a difficult problem.

This paper describes a new method using local orientation estimated with quadrature filters for improving border detection by incorporating temporal information in the border detection. The idea of using temporal information in

C. Taylor, A. Colchester (Eds.): MICCAI'99, LNCS 1679, pp. 410–419, 1999.

segmentation of echocardiographic image sequences is not new; it is proposed and discussed among others in [3,5,8].

2 Method

The overall strategy for segmentation used in this paper is to first compute a border probability image and then use an optimization algorithm to find the most probable segmentation. The objective is to find a border probability image sequence using both spatial and temporal information. In other words, we are looking for border-like structures that are continuous in time. The images in the image sequence are stacked to form a 3D (2D+T) image volume, see Figure 1 a). Consider a slowly moving plane in an image sequence. This is illustrated in Figure 1 b). The angle between the local orientation of a planar structure and the time axis depends on the velocity and continuity in time of the structure. We are searching for borders that are continuous in time, having an orientation approximately orthogonal to the time axis.

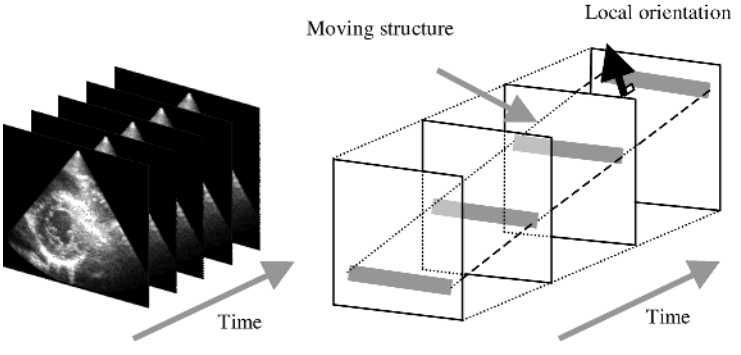

Fig. 1. a) Images are stacked to form an image volume. b) A slowly moving plane in an image sequence. The black arrow indicates the local orientation of the moving structure in the image volume. Note that the orientation of the structure is almost orthogonal to the time axis.

2.1 A 3D Local Orientation Estimate

Mulet-Parada et al. proposed a filter bank consisting of 21 Log-Gabor filters to find a local orientation estimate [8] in an echocardiographic image sequence. An alternative way of estimating local orientation is using quadrature filters and a local orientation tensor concept described by Hans Knutsson [10]. A quadrature filter is a filter with a zero transfer function in one half plane of the frequency domain. The normal vector of that plane is said to be the orientation of the quadrature filter. The quadrature filter is a complex valued filter where the real

part detects boundaries and the imaginary part detects borders. For calculating a local orientation estimate in 3D a set of minimally six quadrature filters is required [9]. The directions of the quadrature filters should be evenly distributed in space. In 3D this is accomplished when each quadrature filter is pointing at nodes of a hemi-icosahedron, as illustrated in Figure 2.

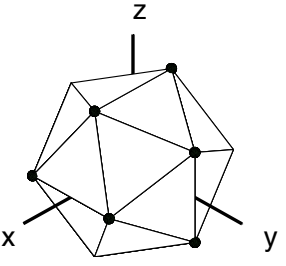

Fig. 2. An Icosahedron, the points on the icosahedron indicates the direction of the quadrature filters.

A tensor describing the local orientation can be constructed as [9]:

$$\mathbf{T_e} = \sum_k q_k \left(\frac{5}{4} \hat{\boldsymbol{n}}_k \hat{\boldsymbol{n}}_k^T - \frac{1}{4} \mathbf{I} \right) \tag{1}$$

Where q_k is the output from quadrature filter k, $\hat{\boldsymbol{n}}_k$ is the direction vector of quadrature filter k, and $\mathbf{I}$ is the identity tensor.

In the 3D case, the tensor is a 3x3 matrix. The eigenvectors and eigenvalues of the tensor describes the nature of the orientation in a local neighborhood. The eigenvector with the largest eigenvalue gives an estimate of the dominant local orientation in the neighborhood. The idea is now that we can suppress structures that are not continuous in time by projecting the estimated orientation vector on a plane normal to the time axis. Remember that a non-moving plane has a normal vector (orientation) orthogonal to the time axis, see Figure 1b. A border probability estimate is therefore:

$$g = \|\lambda_1\| \left\| \begin{bmatrix} 1 & 0 & 0 \\ 0 & 1 & 0 \\ 0 & 0 & 0 \end{bmatrix} \begin{bmatrix} e_{1x} \\ e_{1y} \\ e_{1t} \end{bmatrix} \right\| \tag{2}$$

where g is the border probability. The matrix is a projection matrix (projection on a plane normal to the time axis), λ_1, the vector is the eigenvector corresponding to the largest eigenvalue λ_1 of the tensor $\mathbf{T_e}$.

It is also possible to weight the different border orientations by changing the projection matrix. More important is, however, the ability to distinguish between lines and edges. In our case we are looking for edges that goes from dark to bright (transition between blood pool and myocardium). This is done by only looking at the imaginary part of the eigenvalue.

2.2 Computational Simplification

Instead of calculating a local orientation estimate and projecting the resulting orientation we can directly project the set of quadrature filters. The problem is then reduced to find the local orientation in a 2D plane. Finding local orientation in 2D can be accomplished with only three quadrature filters [9]. In addition, the eigenvalue calculation will be much faster. Note, however, that the quadrature filters are still three dimensional, but fewer filters are required. When four quadrature filters are used in 2D it is possible to directly calculate the local orientation without calculating the eigenvalues and eigenvectors [9].

3 Optimization

The border detection algorithm results in a "border probability" image. From this image we need to find the most probable border using an optimization algorithm. As a foundation for the optimization, the concept of active contours where chosen. Active contours are a common choice for segmenting medical images, since they capture anatomical irregularities well [11]. The border is modeled as a physical string with rigidity and elasticity. The contour is positioned so that its energy is minimized. This approach is usually referred as 'snakes' in the literature [11]. Modeling the border as a string results in the following optimization problem [12]:

$$\min_{f} \int \left(g(f(s)) + \alpha f'(s)^2 + \beta f''(s)^2 \right) ds \tag{3}$$

Where f is the active contour, g is the energy from the border probability image, α and β are elasticity and rigidity, respectively. This optimization problem can not be solved to a guaranteed optimum. Therefore, a reformulation of the optimization problem is required. The problem can be solved by an iterative process such as simulated annealing similar to what Friedland et al. suggested [5]. Iterative algorithms do not give any guarantees about optimality of the result in finite time. Instead, we propose a reformulation of the problem to a combinatorial optimization problem. This reformulation is possible if we can restrict the active contour to a proper discrete function $y(x)$. This restriction can be accomplished by resampling the original image (see section 3.1). The optimization problem in Equation 3 can now be approximated by [12]:

$$\min_{y_i \in 1 \ldots M} \left\{ \begin{array}{l} \sum_{i=1}^{L} \sum_{j=y_{i-1}}^{y_i} \left(\frac{\|y_i - j\|}{\|y_{i-1} - y_i\| + 1} g(i-1, j) + \frac{\|j - y_{i-1}\|}{\|y_{i-1} - y_i\| + 1} g(i, j) \right) + \\ \qquad \sum_{i=1}^{L-1} \alpha (y_i - y_{i+1})^2 + \sum_{i=2}^{L-1} \beta (-y_i + 2y_{i+1} - y_i)^2 \end{array} \right. \tag{4}$$

Where g is the border probability image, α is the elasticity term, β is the rigidity term, L is the number of layers (columns) in the discrete grid, M is the number of

rows in the discrete grid, and the active contour f is represented by the discrete function $f : \{y_i\}$.

The first term of Equation 4 simply describes a sum of linear interpolations in the border probability and the two last terms describes the rigidity and elasticity terms. The main advantage with this new reformulation is that the physical interpretation of treating the contour as a physical string is kept, including rigidity The other advantage is that it can be solved to optimality by a fast dynamic programming algorithm. The problem is solved with an algorithm very similar to Dijkstra's shortest path algorithm. This is possible since y_{i-1} is implicitly known when calculating forward vertices in Dijkstra's algorithm. Details on solving the optimization problem can be found in [12]. Dynamical programming has earlier been used for segmentation of echocardiographic images by among others [3] and [7].

3.1 Resampling

The reformulation of the optimization problem restricts the segmented contour to a proper one-dimensional function $y(x)$. The resampling of the original image was performed before border detection. In the consecutive frames the resampling is performed along the delineated contour in the previous frame (resampling line, indicated in black in Figure 3 below). In this manner the function $y(x)$ can be used to represent the delineated contour for the next frame, assuming a similarity.

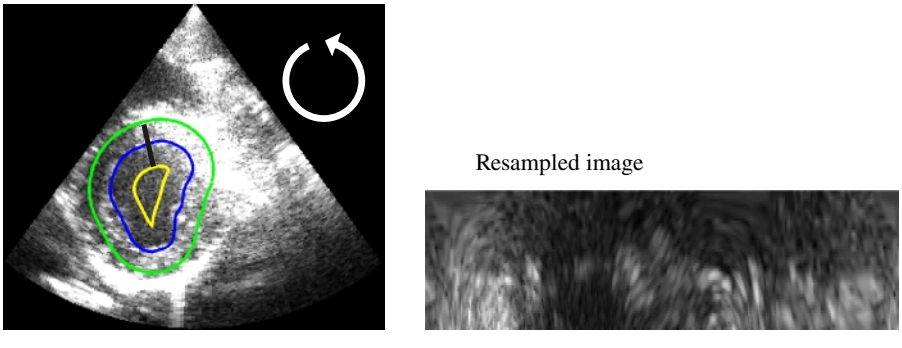

Fig. 3. Left: Original image with resampling direction is indicated by a white arrow. Right: The resampled image.

A delicate question is how to weight temporal and spatial scale. The following idea was used to establish an approximate scale. During one heart beat in a normal heart a point on the endocardium moves approximately 10 mm before it returns to its original position. There are approximately 50 frames in one heartbeat. Therefore 50 frames should correspond to 10 mm.

4 Validation

The segmentation performance using gradient based border detection and local orientation border detection was compared. The optimization parameters where kept constant ($\alpha = 0.001$ and $\beta = 0.005$). The border probability image was normalized prior to the optimization process. For gradient based border detection a 5x10 median filter, followed by two orthogonal gradient filters (1 0 -1) were applied. The orientation filter size was 9x9x9 pixels with a bandwidth of one octave and a center-frequency of $\pi/5$.

First, an artificial image sequence consisting of a moving border in a fair amount of noise was used to evaluate the two border detection methods. The image sequence was 100x100x9 pixels, and the amplitude of the border was 1/5 in a fully developed Gaussian multiplicative speckle noise. The phantom image sequence is shown in Figure 5.

To quantitatively assess the accuracy of the segmentation process, image sequences from three normals and two patients were used. The images were acquired from parasternal short axis view. The number of frames per heartbeat were not resampled, and varied between 39 to 70. The original image was resampled to 50x300 pixels (orthogonal to resampling line and along resampling line respectively). User interaction was limited to setting region of interest on the first image. The same region of interest was used for both border detection methods. The segmentation result was compared with a manual delineation performed by two different observers on 10 images per image sequence. Papillary muscles where included in the delineation, if they where connected to the wall in the imaged plane.

Quantitative analysis of segmentation performance on *in-vivo* data is a difficult task since there is no gold standards available [1]. Two measures were used for comparison, delineated cavity area and symmetrical difference. Symmetric difference is an error metric defined as the area of a pixelwise XOR comparison on those pixels enclosed by the different segmentations, see Figure 4. The difference was calculated in 10 images per heart beat evenly distributed in time and in six segments in each image.

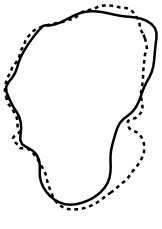

Fig. 4. The symmetric difference between two delineations — dashed and solid lines respectively, is marked in gray color.

5 Results

In the case of the phantom, no consistent border could be found at all with the gradient border detection algorithm. When temporal information was included, the border could be detected with good accuracy, see Figure 5.

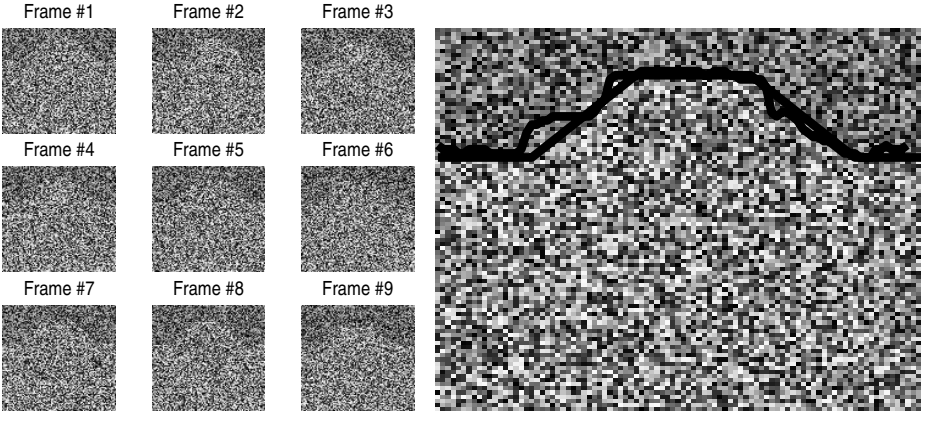

Fig. 5. Left: Test image sequence with a slowly moving border with a fair amount of noise. Right: Border detected in frame #5 of the image sequence. The 'straight' line is the true border and the 'wigged' line is the border detected by the algorithm.

For the *in-vivo* image sequences, cavity area was used for determination of systematic errors and symmetric difference was used to determine in which segment the differences were most pronounced. In one of the image sequences with poor image quality it was not possible to perform fully automatic segmentation using the gradient border detection algorithm, while the local orientation succeeded well. This sequence was removed from further statistical analysis. The differences in mean cavity area and mean symmetric difference in different segments for the two border detection methods compared to the two observers are illustrated in Figure 6. A Bland Altman analysis [13] was performed to find out if manual segmentation could be replaced with automatic segmentation, see Figure 7.

6 Discussion

The border detection method proposed in this paper is easily expanded to higher dimensions such as 3D+T. Images from different modalities can easily be used such as MRI or 3D ultrasound. In 3D+T, the computational simplification presented is extra valuable since it reduces the number of quadrature filters required from 24 to 6. One improvement applicable to the segmentation process proposed

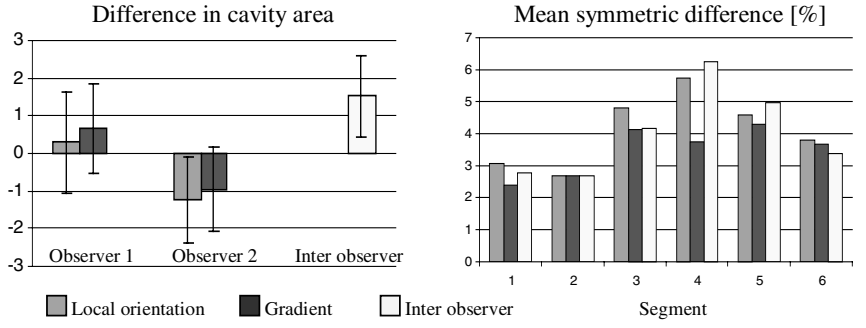

Fig. 6. Left: The difference in cavity area measured with the two border detection methods compared to the two observers. Note the systematic difference between the two observers. Right: Symmetric difference in different segments for the two border detection methods compared to manual delineation. The segments are anterior wall (1), anterior septal (2), posterior septal (3), posterior (4), posterior lateral (5), and anterior lateral (6). As a reference inter-observer symmetric difference is also plotted.

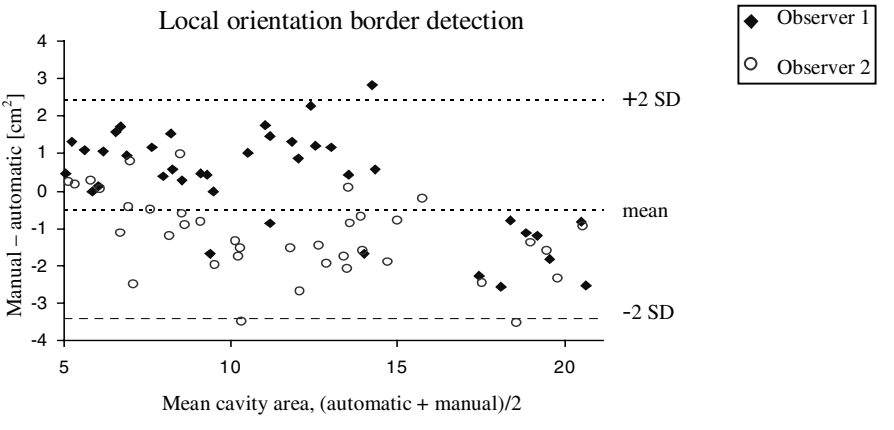

Fig. 7. Bland Altman plot where segmentation using local orientation border detection is compared with the manual delineation by the two observers.

in this paper would be to optimize the contour for all frames in parallel (i.e. a 2D+T deformable model for the entire image volume) [14]. Unfortunately the reformulation of the optimization algorithm proposed here can then no longer be used and an iterative algorithm has to be used for the optimization.

7 Conclusion

The fact that endocardial border detection of echocardiograhic image sequences is a difficult task is clearly illustrated with the large inter-observer difference. Automatic segmentation has the advantage of good reproducibility. Therefore automatic segmentation could be a method to reduce variability. Further investigation is necessary before it is possible to say that automatic segmentation statistically can replace manual segmentation. The mean symmetric difference for the six segments corresponds well to the symmetric difference for inter-observer delineations. This suggests that the differences in measured cavity area between computer and manual delineations arose in the same segments as where the human observers had difficulties. It can be concluded that when temporal information is included weak and incomplete boundaries (such as in the phantom and one of the image sequences) can be found where gradient based border detection fails.

References

1. V. Chalana and Y. Kim: A methodology for evaluation of boundary detection algorithms on medical images. IEEE Trans Med Imaging, vol. 16, pp. 642–52, 1997. 410
2. J. M. B. Dias and J. M. N. Leitõ: Wall Position and Thickness Estimation from Sequences of Echocardiographic Images, IEEE Transactions on Medical Imaging, vol. 15, pp. 25-38, 1996. 410
3. B. B. Luc Maes, Paul Suetens, Frans Van de Werf: Automated contour detection of the left ventricle in short axis view in 2D echocardiograms, Machine Vision and Applications, vol. 6, pp. 1-9, 1993. 410, 411, 414
4. J. W. Klingler, Jr., C. L. Vaughan, T. D. Fraker, Jr., and L. T. Andrews: Segmentation of echocardiographic images using mathematical morphology, IEEE Trans Biomed Eng, vol. 35, pp. 925-34, 1988. 410
5. N. Friedland and D. Adam: Automated ventricular boundary detection from sequential ultrasound images using simulated annealing, IEEE Transactions on Medical Imag, vol. 4, pp. 344-353, 1989. 410, 411, 413
6. A. Chakraborty, L. H. Staib, and J. S. Duncan: Deformable Boundary Finding in Medical Images by Integrating Gradient and Regional Information, IEEE Transactions on Medical Imaging, vol. 15, pp. 859-870, 1996. 410
7. M. Unser, G. Pelle, P. Brun, and M. Eden: Automated Extraction of Serial Myocardial Borders from M-Mode Echocardiograms, IEEE Transactions on Medical Imaging, vol. 8, pp. 96-103, 1989. 410, 414
8. M. Mulet-Parada and J. A. Noble: 2D+T Acoustic Boundary Detection in Echocardiography presented at MICCAI-98, Cambridge, 1998. 411

9. G. Granlund and H. Knutsson: Signal Processing for Computer Vision, Linköping: Kluwer Academic Publishers, 1995. 412, 413
10. H. Knutsson: Representing local structure using tensors, presented at the 6th Scandinavian Conferance on Image Analysis, pp 244-251, Oulo, Finland, June 1989. 411
11. T. McInery and D. Terzopoulos: Deformable models in medical image analysis: a survey, Medical Image Analysis, vol. 1(2), 1996. 413
12. E. Brandt: Segmentation Techniques for Echocardiographic Image Sequences, LiTH-ISY-EX-1934, 1998, Department of Electrical Engineering, Linköpings Universitet, Sweden. 413, 414
13. J. M. Bland and G. D. Altman: Statistical methods for assessing agreement between two methods of clinical measurent, The Lancet, February 8, pp. 307-310, 1986. 416
14. D. Kucera and R. W. Martin: Segmentation of sequences of echocardiographic images using a simplified 3D active contour model with region-based external forces, Comput Med Imaging Graph, vol. 21, pp. 1-21, 1997. 418